HEAVY FLAVOUR PRODUCTION IN P$\bar{P}$ COLLISIONS

W.L. van Neerven
Instituut-Lorentz
University of Leiden
P.O. Box 9506
2300 RA Leiden, The Netherlands

ABSTRACT

We would like to report on a recent calculation of the order α_S correction to heavy flavour production. Here only the contribution to the gluon-gluon fusion mechanism has been taken into account. Results are given for total as well as differential distributions for the range of $p\bar{p}$ collision energies available at CERN and Fermi-Lab. A comparison is made with the recent data from the UA1 collaboration.

Recently two groups have calculated the order α_s corrections to heavy flavour production [1,2]. These calculations are very important for the search of the top quark and the study of the properties of bottom and charmed quarks. There are two important contributions to heavy flavour production. The first one, which is theoretically as well as experimentally better understood, is the process where the heavy flavours appear as the decay products of the W and Z bosons. The latter are produced via the Drell-Yan mechanism in $p\bar{p}$ collisions. However this source of heavy flavour production is only important for the top quark [3] provided its mass satisfies the relation $m_t < M_Z/2$ or $m_t < M_W - m_b$. In the second and dominant mechanism the heavy quarks are directly created via parton-parton collisions. The interactions among these partons are described by perturbative QCD [4]. In lowest order of the strong coupling constant g there are two parton-parton subprocesses which are quark-antiquark annihilation and gluon-gluon fusion i.e.,

$$q+\bar{q} \rightarrow Q+\bar{Q} \tag{1}$$

$$g+g \rightarrow Q+\bar{Q} \tag{2}$$

Both lowest $O(\alpha_s^2)$ processes have been extensively analyzed in the literature [4]. The analysis reveals that

a. The heavy quarks are mainly produced in the centre of the rapidity plot for the cross section $d\sigma/dy$ (i.e. $|\Delta y| \leq 1$).
b. The average p_t is of the order of the heavy flavour mass m and $d\sigma/dp_t$ falls rapidly to zero as $p_t > m$.
c. The gluon-gluon fusion process (2) is the dominant production mechanism for $c\bar{c}$ and $b\bar{b}$ production. However for $t\bar{t}$ production the quark-antiquark annihilation process (1) becomes important too and the corresponding cross section is of the same order of magnitude as the one obtained from process (2).

It will be now important to see how the above conclusions are changed if we include the $O(\alpha_s)$ corrections. The $O(\alpha_s)$ corrections to the processes in (1) and (2) receive the following contributions.

1. One loop corrections to the processes (1) and (2).
2. Initial and final state gluon radiation in processes (1) and (2). They are given by the reactions

$$q+\bar{q} \to Q+\bar{Q}+g \quad (3)$$

$$g+g \to Q+\bar{Q}+g \quad (4)$$

3. In addition one gets a new production mechanism in order α_s^3 i.e. quark-gluon fusion

$$g+q(\bar{q}) \to Q+\bar{Q}+q(\bar{q}) \quad (5)$$

All these corrections have been calculated in ref. 1 whereas we have limited ourselves to the gluon-gluon fusion mechanism only[2]. However in practice it turns out that the contribution from the latter process constitutes the bulk of the whole $O(\alpha_s)$ correction, even in the case of top production. Our aim is now to compute the double differential parton cross section corresponding to the above processes. After convolution with the input parton distribution functions one obtains the hadronic cross sections which are of experimental interest. While calculating the Feynman diagrams one encounters three types of singularities i.e. Ultraviolet (UV), infrared (IR) and collinear (C) divergences. They were all regularized by using the method of n-dimensional regularization. Since the heavy quarks are massive one has to perform mass renormalization for which we choose the on shell scheme. For coupling constant renormalization we have taken the $\overline{MS}$ scheme. However this scheme leads to large corrections of the type $\ln Q^2/m_f^2$ when $Q^2 \gg m_f^2$ or $Q^2 \ll m_f^2$. Here Q^2 denotes the renormalization scale. The corrections can be attributed to the internal heavy fermion loop (mass $= m_f$) contributions. In order to avoid these large corrections one can choose a scheme where these heavy fermion contributions are decoupled. In this talk we shall present results calculated in the latter scheme. In order to give an insight in the various contributions we have split the parton cross section in a virtual, soft and hard gluon part. After having performed mass and coupling constant renormalization we have to cancel the IR singularities which appear in the virtual as well as soft gluon cross section. Finally we are left with the C divergences which show up in the sum of the virtual + soft as well as hard gluon cross section. They are removed by mass factorization for which we have chosen the $\overline{MS}$ scheme. In this way we obtain the reduced parton cross section which depends on the renormalization scale Q^2 as well as the mass factorization scale μ^2. Both scales were put to be equal to m^2.

The size of the radiative corrections depends on the reduced parton cross section as well as input parton (in our example gluon) distribution functions. In order to get some insight in the origin of the large correction terms we first discuss the parton cross section. The total parton cross section can be expressed in scaling functions $f_{ij}^{(k)}(\rho)$ as follows [1]

$$\hat{\sigma}_{ij}(s,m^2) = \frac{\alpha_s^2(\mu^2)}{m^2} [f_{ij}^{(0)}(\rho) + 4\pi\alpha_s(\mu^2) f_{ij}^{(1)}(\rho) + \ldots], \qquad (6)$$

where $\rho = 4m^2/s$. The above expression holds provided we have chosen a coupling constant renormalization schema where the heavy fermions are decoupled and the fermion loop masses m_f are neglected with respect to the heavy flavour mass m. In fig. 1 we have plotted $f_{gg}^{(0)}(\rho)$ (Born contribution) as well as the order α_s contribution $f_{gg}^{(1)}(\rho)$ due to the soft + virtual as well as hard gluon parts. Since the threshold region $1<\rho^{-1}<2$ is extremely important for heavy flavour production we also made a close-up of fig. 1 see fig. 2. The results presented above are in agreement with those given in ref. 1. The above figures reveal some large corrections appearing in the various regions of ρ. They can be found in

a. <u>Large s (ρ^{-1}) region.</u>
   In this region there is a large plateau in the cross section due to the exchange of gluons (massless vector bosons) in the t-channel (fig. 3a, gluon splitting graph).

b. <u>Threshold region $s \to 4m^2$ ($\rho^{-1} \to 1$).</u>
   This region is dominated by two mechanisms. b1) The Coulomb singularity present in the virtual part of the cross section which is due to the exchange of gluons between massive quarks in the final state (fig. 3b). b2) The soft tail of the hard gluon bremsstrahlung spectrum which can be traced back to the flavour excitation graph in fig. 3c.

In order to make realiable predictions one must get these large corrections under control. It turns out that the threshold region is dominated by the soft gluon radiation terms which behave like $\ln^i(1-\rho)$ if $\rho \to 1$. As is shown in refs. 1,2 the leading terms can be exponentiated providing us with a better estimate of the higher order α_s corrections to the hadronic cross section.

Besides the parton cross section the size of the radiative corrections is also determined by the input parton distribution function $f_i^h(x,\mu^2)$. Here i denoted the parton and h refers to the hadron where the parton i is originating from. The total hadronic cross section is given by

$$\sigma_{tot}(s,\mu^2) = \sum_{i,j} \int_{4m^2/s}^{1} dx\ \Phi_{ij}(x,\mu^2)\hat{\sigma}_{ij}(xs,\mu^2). \tag{7}$$

The parton flux $\Phi_{ij}(x,\mu^2)$ is defined by

$$\Phi_{ij}(x,\mu^2) = \int_0^1 dx_1 \int_0^1 dx_2\ \delta(x-x_1x_2) f_i^{h_1}(x_1,\mu^2) f_j^{h_2}(x_2,\mu^2). \tag{8}$$

In the case of the gluon fusion process (2), (4) we observe that the size of the radiative correction is mainly determined by the small x region where the gluon flux gets very large. This follows from the behaviour of the gluon distribution function $f_g^h(x) \sim \frac{1}{x}(1-x)^5$. Therefore the threshold behaviour of the parton cross section becomes very important because xs approaches $4m^2$ if x gets small. This is in particular the case for top production. Since the gluon distribution function rapidly drops off to zero if $x \to 1$ the plateau effect $(\rho^{-1} > 10)$ of the parton cross section gets suppressed. It turns out that the plateau region is unimportant for top production. However in the case of charm and bottom production the cross section receives some contributions of the latter region too.

In table 1 and 2 we show the hadronic total cross section for bottom and top production. For the input parton distribution functions we took the EHLQ parametrization with $\Lambda=0.2$ GeV/c. The two loop corrected

Table 1: Total $p\bar{p}$ cross section (all units in μb) for b-quark production $m_b = 5.0$ GeV/c, $\alpha_s(m_b)=0.190$ for both $q\bar{q}$, gg and $n_f = 5$; see ref. 5.

$\sqrt{S}$(TeV)	$q\bar{q}$ $O(\alpha_s^2)$	gg $O(\alpha_s^2)$	gg $O(\alpha_s^3)$
0.63	0.22	5.3	5.0
1.8	0.31	16	18

running coupling constant was taken over from eq. 10 in ref. 5. As already has been mentioned above both the factorization scale as well as the renormalization scale were put to be equal to m^2. From table 1 (bottom production) we infer that the gluon gluon fusion process overwhelms all the other production mechanisms so that we do not have to consider them including their radiative corrections. The same holds for charm production. However in the case of top production the quark-antiquark fusion becomes important too, see table 2. However from ref. 1 we infer that the order α_s corrections (3) and the contribution of the quark-gluon fusion process (4) are small. This one can see if we compare the complete $O(\alpha_s)$ corrected

Table 2: Total $p\bar{p}$ cross section (all units in nb) for t-quark production $\alpha_s(40) = 0.125$, $\alpha_s(80) = 0.112$ for both $q\bar{q}$, gg; and $n_f=5$, see ref. 5.

$m_t(\mathrm{GeV}/c^2)$	$\sqrt{S}(\mathrm{TeV})$	$q\bar{q}\ O(\alpha_s^2)$	$gg\ O(\alpha_s^2)$	$gg\ O(\alpha_s^3)$	$q\bar{q}+gg+qg$ $(O(\alpha_s^2)+O(\alpha_s^3))$
40.0	0.63	0.29	0.26	0.21	0.84
40.0	1.8	1.03	6.5	4.1	12.4
80.0	0.63	0.009	0.0008	0.0008	0.013
80.0	1.8	0.095	0.16	0.10	0.375

cross section [1,5] (last column of table 2) with the result obtained from process (1), (2) and (4). Omitting the contribution from process (3) and (5) only leads to an error of about 10% which is within the uncertainty of our prediction due to the running coupling constant (about 10%) and the input parton distribution functions.

Besides the total cross sections we have also computed the full $d\sigma/dp_t$ distributions for bottom ($\sqrt{S}$=0.63 TeV, fig. 4) and top ($\sqrt{S}$=1.8 TeV, fig. 5) production. Here p_t is the transverse momentum of one of the outgoing heavy flavours. The plots show a K-factor $K(p_t)$ which varies very smoothly as a function of p_t. We have observed a very small increase in K when p_t gets larger. However this is hardly visible in a logarithmic plot. The same we observe for the rapidity (y) distribution $d\sigma/dy$ (figs. 6,7). However in the case of bottom production the order α_s correction to $d\sigma/dy$ drops off much faster at large y than the Born contribution.

Finally we want to present our result (fig. 8) for the distribution

$$\sigma(p_{t,min}) = \int_{p_{t,min}}^{p_{t,max}} d\,p_t \int_{|y|<1.5} dy \frac{d^2\sigma}{dp_t dy} , \tag{9}$$

which has recently been measured by the UA1 group [6] for bottom production. From fig. 8 we observe that our curve is very close to the data provided we take the factorization/normalization scale equal to m_b^2. If one takes as scale $\mu^2 = m_b^2+p_t^2$ then the curve drops off much faster as a function of $p_{t,min}$. This is what probably happens with the theoretical distribution shown in fig. 3 of ref. 6. It indicates that these types of distributions are very sensitive to the factorization scale which means that higher order corrections are important too.

References

1) P. Nason, S. Dawson, and R.K. Ellis, Nucl. Phys. B303 (1988) 607.
2) W. Beenakker, H. Kuijf, W.L.van Neerven and J. Smith, Leiden Preprint to be published in Phys. Rev. D.
3) A. Ali, B. van Eijk and I. ten Have, Nucl. Phys. B291 (1987) 1.
4) See the list of references in 1) and 2).
5) G. Altarelli, M. Diemoz, G. Martinelli, and P. Nason, Nucl. Phys. B308 (1988) 724.
6) C. Albajar et al., Phys. Lett. B213 (1988) 405.

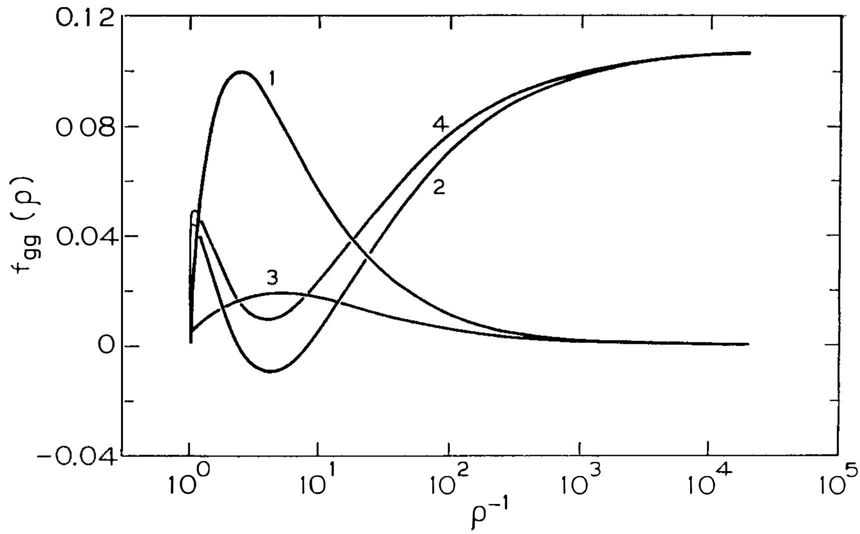

Fig. 1. Plot of the scaling functions $f_{gg}^{(0)}(\rho)$ and $f_{gg}^{(1)}(\rho)$ appearing in (6). 1. $f_{gg}^{(0)}(\rho)$, Born term. 2. $f_{gg}^{(1)}(\rho)$, hard gluon part. 3. $f_{gg}^{(1)}(\rho)$, virtual + soft gluon part. 4. $f_{gg}^{(1)}(\rho)$, hard + virtual + soft.

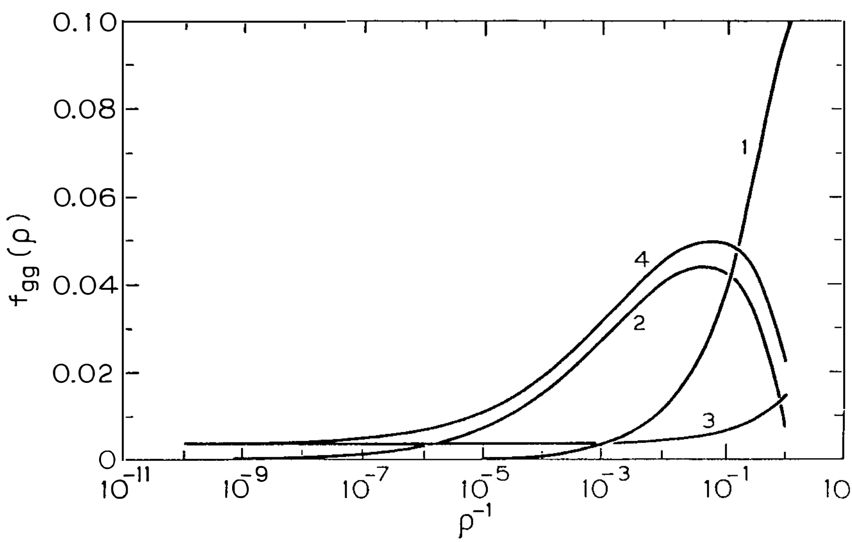

Fig. 2. Close-up of fig. 1 for the region $1<\rho^{-1}<2$.

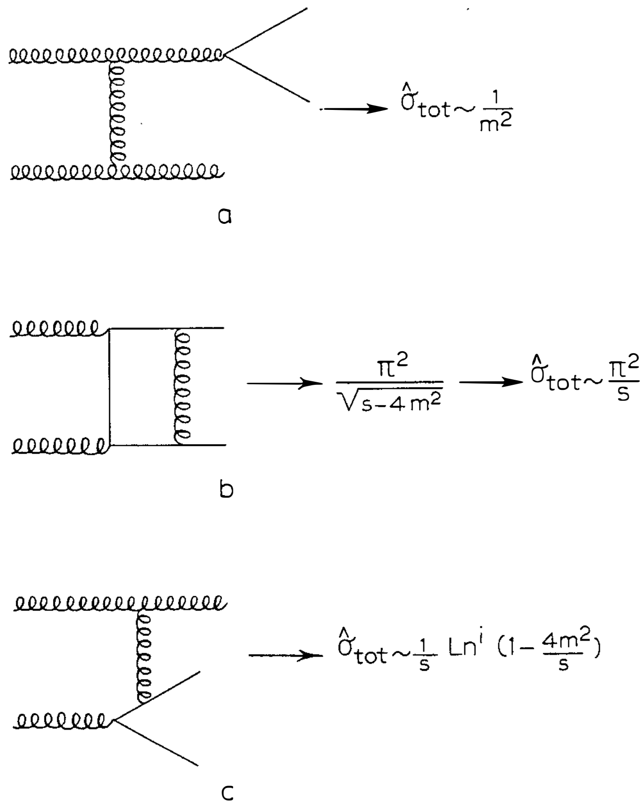

Fig. 3. Dominant production mechanisms contributing to $f_{gg}^{(1)}(\rho)$.

a. gluon splitting;

b. virtual gluon exchange between final state fermions;

c. flavour excitation.

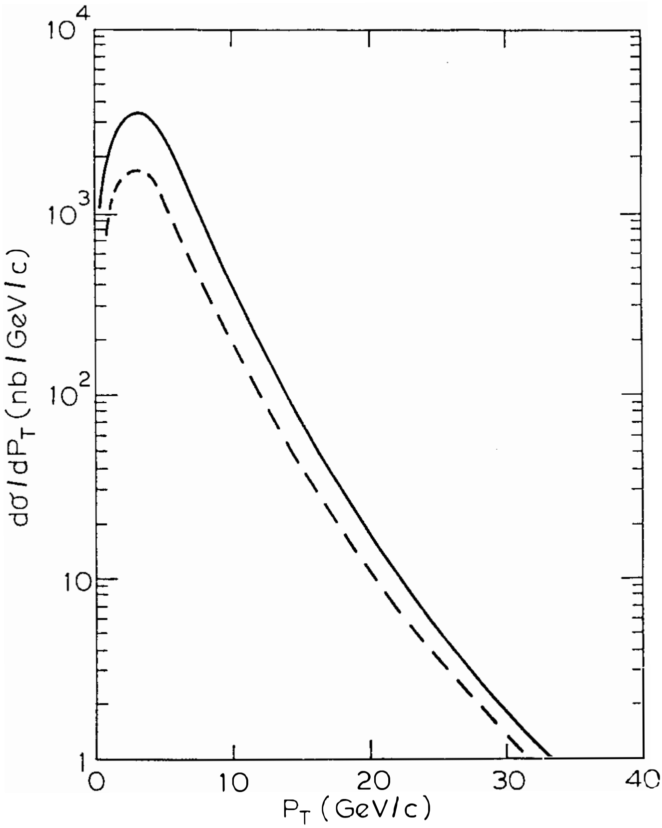

Fig. 4. $d\sigma/dp_t$ for b-quark production (m_b=5.0 GeV/c^2) at $\sqrt{S}$ =0.63 TeV. Dashed line: $O(\alpha_s^2)$ cross section. Solid line: sum of the $O(\alpha_s^2)$ and $O(\alpha_s^3)$ cross sections.

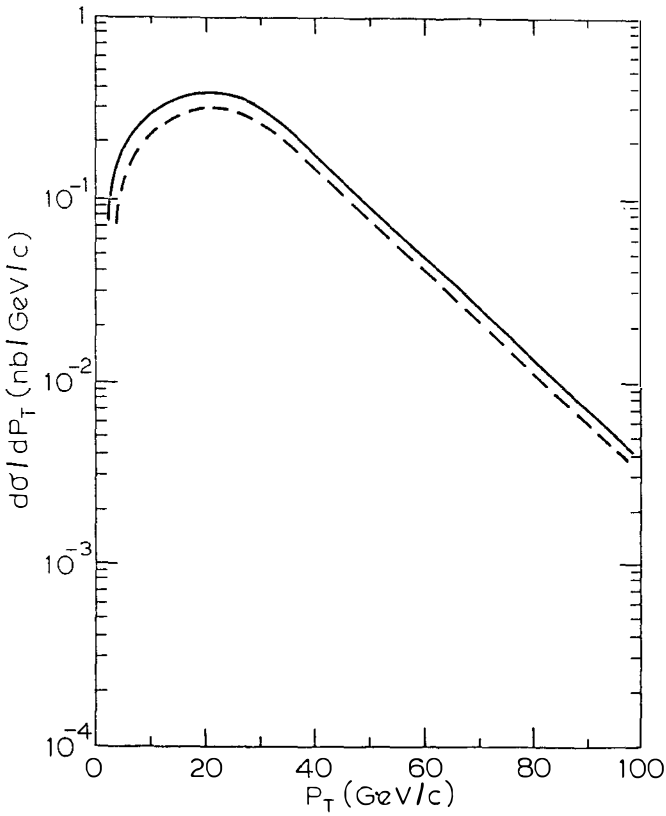

Fig. 5. $d\sigma/dp_t$ for t-quark production (m_t=40.0 GeV/c^2) at $\sqrt{S}$=1.8 TeV. Dashed line: $O(\alpha_s^2)$ cross section. Solid line: sum of the $O(\alpha_s^2)$ and $O(\alpha_s^3)$ cross sections.

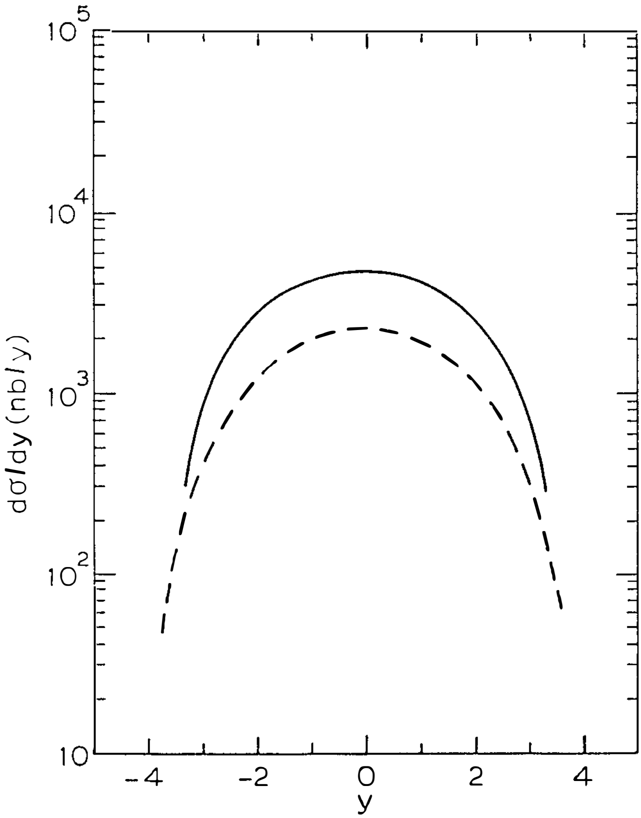

Fig. 6. $d\sigma/dy$ for b-quark production (m_b=5.0 GeV/c^2) at $\sqrt{S}$=0.63 TeV. Dashed line: $O(\alpha_s^2)$ cross section. Solid line: sum of the $O(\alpha_s^2)$ and $O(\alpha_s^3)$ cross sections.

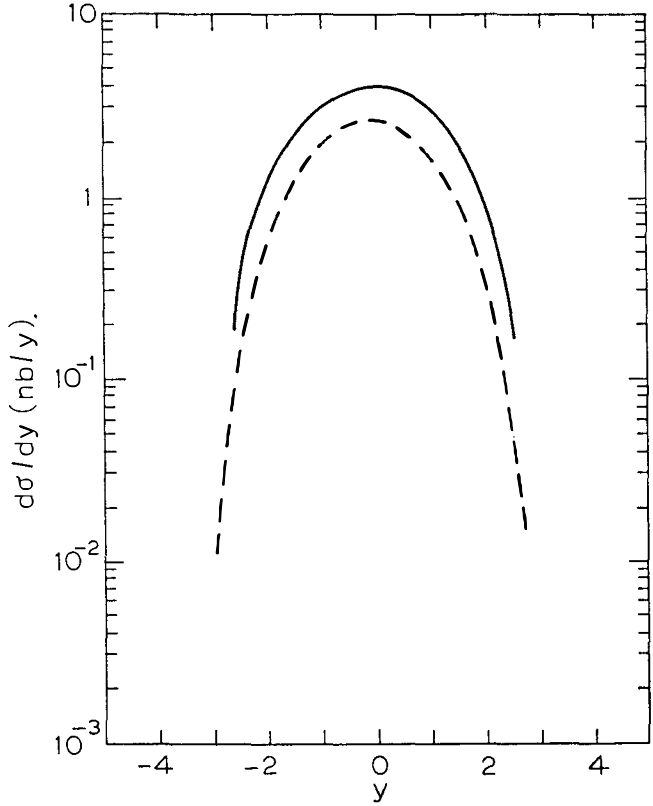

Fig. 7. dσ/dy for t-quark production (m_t=40.0 GeV/c^2) at $\sqrt{S}$=1.8 TeV. Dashed line: $O(\alpha_s^2)$ cross section. Solid line: sum of the $O(\alpha_s^2)$ and $O(\alpha_s^3)$ cross sections.

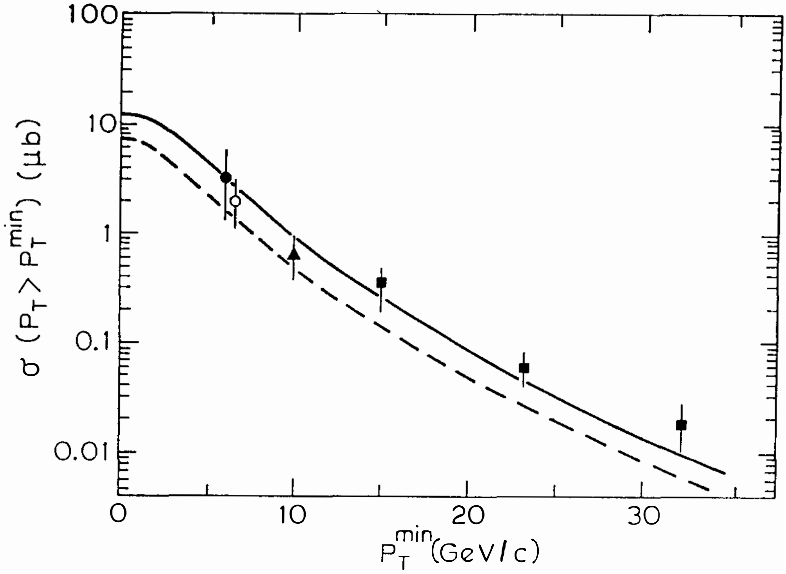

Fig. 8. The inclusive bottom cross section in $p\bar{p}$ collisions at $\sqrt{S}=0.63$ TeV for $p_t(b) > p_{t,min}$ and $|y(b)| < 1.5$ as a function of $p_{t,min}$.
Dashed line: $O(\alpha_s^2)$ cross section. Solid line: sum of the $O(\alpha_s^2)$ and $O(\alpha_s^3)$ contributions to the cross section in in eq. 9.